Optica Applicata, Vol. XLVII, No. 1, 2017
DOI: 10.5277/oa170106

Effects of inner and outer scale on beam spreading for a Gaussian wave propagating through anisotropic non-Kolmogorov turbulence

CHAO GAO, XIAOFENG LI*

School of Astronautics and Aeronautic, University of Electronic Science and Technology of China, 2006 Xiyuan Avenue, 611731 Chengdu, China

*Corresponding author: lxf3203433@uestc.edu.cn

Experimental results and empirical research have shown that atmospheric turbulence can present the anisotropic property not only at a few meters above the ground but also at high altitudes of up to several kilometers. This paper investigates beam spreading for a Gaussian wave propagating along a horizontal path in weak anisotropic non-Kolmogorov turbulence. Mathematical expressions for the long-term beam spreading radius were obtained based on the generalized von Kármán spectrum for anisotropic turbulence. The final model includes an anisotropic factor, which parameterizes the asymmetry of a turbulence cell, the spectral power law for non-Kolmogorov turbulence, the inner and outer scale of turbulence, and other essential optical parameters of a Gaussian wave. Numerical simulations indicate that the long-term beam spreading radius decreases with an increase in the anisotropic factor. We also analyze how the geometrical optics approximation may cause large errors for a small spectral power law value.

Keywords: anisotropy, Gaussian wave, long-term spreading radius, non-Kolmogorov turbulence, inner and outer scales of turbulence.

1. Introduction

Propagation of optical beams through the atmosphere has been attracting increasing attention in the field of wireless communication. The atmosphere is a special type of inhomogeneous flow, with a large quantity of complicated and rule-less turbulence [1, 2]. Atmospheric turbulence can damage the information carried by an optical beam and decrease the performance of wireless communication systems. Consequently, active research has been conducted in the last few decades on the effects of atmospheric turbulence. Beam spreading, one of usual consequences of atmospheric turbulence, causes finite optical beams to experience random deflections while propagating. The long-term spreading radius characterizes this phenomenon statistically [3, 4].

Many power spectrum models of refractive-index fluctuations have been proposed to analyze the long-term spreading radius, and satisfy different conditions. Generally

speaking, these turbulence power spectrum models can be classified into Kolmogorov and non-Kolmogorov models. The former have a fixed power law value 11/3, while the latter allow the power law value to vary over 3–4 [5–7]. Most non-Kolmogorov models can be generalized from their corresponding Kolmogorov models, and thus the Kolmogorov models can be regarded as specific cases of the non-Kolmogorov models. In the past few decades, experimental results and empirical research have pointed out that the atmospheric turbulence can be anisotropic not only at several meters above the ground but also at high altitudes of up to 25 km [8, 9]. Circularly symmetric and scale -dependent anisotropic spectra have been proposed to investigate the effects of anisotropic turbulence on irradiance scintillation, angle-of-arrival fluctuation, *etc*. [10–16].

This paper investigates the mathematical expression of the long-term beam spreading radius for a Gaussian wave propagating in anisotropic turbulence along a horizontal path, without applying the geometrical optics approximation (GOA). GOA is widely used to reduce the expressions, especially for the classical Kolmogorov cases [17]. However, GOA ignores diffraction effects, and is generally limited to situations where the Fresnel's scale l_{F} is much less than the inner scale of turbulence l_0 [1]. When $l_{\mathrm{F}} > l_0$, GOA-based models can deviate significantly, and are improper for expression reduction. The rest of the paper is organized as follows. Section 2 introduces the theoretical models dealing with the long-term spreading radius for a Gaussian wave and the generalized von Kármán spectrum for anisotropic turbulence. Section 3 derives the detailed expression reduction, and numerical simulations are presented in Section 4. Our conclusions are given in Section 5.

2. Theoretical models

2.1. Generalized von Kármán spectrum for anisotropic turbulence

The generalized von Kármán spectrum for anisotropic turbulence takes the form [11]

$$\Phi_{\mathrm{n\_iso}}(\kappa) = A(\alpha) C_n^2 (\kappa^2 + \kappa_{\mathrm{L}}^2)^{-\alpha/2} \exp\left(-\frac{\kappa^2}{\kappa_{\mathrm{H}}^2}\right) \tag{1}$$

where $\kappa = \sqrt{\kappa_x^2 + \kappa_y^2 + \kappa_z^2}$ is the scalar spatial wave number related to the size of the turbulence cell with components κ_x, κ_y, and κ_z in the x-, y-, and z-directions, respectively; $\alpha \in (3, 4)$ is the general spectral power law value, $A(\alpha)$ is a function related to α

$$A(\alpha) = \frac{\Gamma(\alpha - 1)}{4\pi^2} \cos\left(\frac{\alpha\pi}{2}\right) \tag{2}$$

where Γ denotes the gamma function. Both κ_{H} and κ_{L} are cut-off wave numbers related to the turbulence inner scale l_0 and outer scale L_0

$$\begin{cases} \kappa_{\mathrm{L}} = \dfrac{2\pi}{L_0} \\ \kappa_{\mathrm{H}} = \dfrac{C(\alpha)}{l_0} \\ C(\alpha) = \left[\dfrac{\pi(3-\alpha)}{3} A(\alpha)\, \Gamma\left(\dfrac{3-\alpha}{2}\right) \right]^{1/(\alpha-5)} \end{cases} \tag{3}$$

and C_n^2 in (1) is the generalized atmospheric structure parameter.

Figure 1 depicts $A(\alpha)$ and $C(\alpha)$ as a function of the spectral power law α. It can be seen that $A(\alpha)$ increases monotonically from $\lim_{\alpha \to 3} A(\alpha) = 0$ while $C(\alpha)$ decreases monotonically. Thus, the cut-off wave number at high κ_{H} decreases with an increase in the spectral power law α.

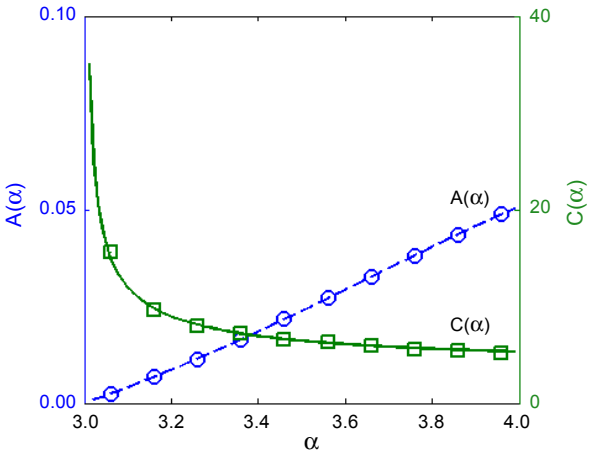

Fig. 1. $A(\alpha)$ and $C(\alpha)$ as a function of the spectral power law.

For the anisotropic non-Kolmogorov turbulence, suppose that the anisotropy exists only along the direction of propagation (z-direction) of the beam. Let a dimensionless quantity ζ_{e} be the anisotropic factors. When ζ_{e} are equal to 1, the turbulence becomes isotropic. When ζ_{e} increases, the anisotropic property of turbulence becomes apparent.

Similar to Eq. (1), the generalized von Kármán spectrum for the anisotropic turbulence takes the following form [11]:

$$\Phi_{\mathrm{n\_iso}}(\kappa') = A(\alpha) C_n^2 \zeta_{\mathrm{e}}^2 (\kappa'^2 + \kappa_{\mathrm{L}}^2)^{-\alpha/2} \exp\left(-\frac{\kappa'^2}{\kappa_{\mathrm{H}}^2}\right) \tag{4}$$

where $\kappa' = \sqrt{\zeta_{\mathrm{e}}^2(\kappa_x^2 + \kappa_y^2) + \kappa_z^2}$.

For convenience of analysis, this paper assumes that the beam propagates along the z-axis. Thus, κ_z can be ignored according to the Markov approximation. The Markov approximation supposes the atmospheric turbulence to be layered along the propagation path while the transmission of energy only happens over these planes orthogonal to the propagation path in the inertial subrange [11, 13]. Under the Markov approximation, the refractive index is uncorrelated between any pair of points along the direction of propagation. Hence, κ_z in Eq. (4) is assigned to zero in the following analyses, and

$$\Phi_n(\kappa) = A(\alpha) C_n^2 \zeta_{\mathrm{e}}^{2-\alpha} \left(\kappa^2 + \frac{\kappa_{\mathrm{L}}^2}{\zeta_{\mathrm{e}}^2} \right)^{-\alpha/2} \exp\left(-\frac{\zeta_{\mathrm{e}}^2 \kappa^2}{\kappa_{\mathrm{H}}^2} \right) \tag{5}$$

2.2. Long-term spreading radius for a Gaussian beam

Long-term beam spreading is the consequence of turbulence-induced spreading beyond laser diffraction effects over a long time period, and also contains the effects of beam wander. The long-term spreading radius for a Gaussian beam at the receiver plane can be modeled as $W_{\mathrm{lt}} = W\sqrt{1+T}$ [1], where W is the beam radius in a vacuum at the receiver $W = W_0\sqrt{\Theta_0^2 + \Lambda_0^2}$ and

$$T = 4Lk^2\pi^2 \int_0^1 \mathrm{d}\xi \int_0^{+\infty} \kappa \Phi_n(\kappa) \left[1 - \exp\left(-\frac{L\Lambda\xi^2\kappa^2}{k} \right) \right] \mathrm{d}\kappa \tag{6}$$

and L is the length along the propagation path, $k = 2\pi/\lambda$ is the angular wave number with the wavelength λ of the Gaussian beam, ξ is the normalized path coordinate, Λ is the optical parameter of the Gaussian beam at the receiver

$$\Lambda = \frac{\Lambda_0}{\Theta_0^2 + \Lambda_0^2} \tag{7}$$

and Θ_0 is the curvature parameter of the Gaussian beam at the transmitter, Λ_0 is the Fresnel ratio of the Gaussian beam at the transmitter

$$\begin{cases} \Theta_0 = 1 - \dfrac{L}{R_0} \\ \Lambda_0 = \dfrac{2L}{kW_0^2} \end{cases} \tag{8}$$

and R_0 is the phase front radius of the Gaussian beam at the transmitter, and W_0 is the waist size of the Gaussian beam.

3. Formula reduction

This section mainly discusses the reduction of Eq. (6). Using the Maclaurin series (or the Taylor series centered at zero), we get [18]

$$1 - \exp\left(-\frac{L\Lambda\xi^2\kappa^2}{k}\right) = -\sum_{n=1}^{+\infty}\frac{1}{n!}\left(-\frac{L\Lambda\xi^2\kappa^2}{k}\right)^n \tag{9}$$

Substituting Eq. (9) into Eq. (6), T is rewritten as

$$T = -4Lk^2\pi^2\sum_{n=1}^{+\infty}\frac{1}{(2n+1)n!}\left(-\frac{L\Lambda}{k}\right)^n\int_0^{+\infty}\kappa^{2n+1}\Phi_n(\kappa)\mathrm{d}\kappa \tag{10}$$

If we only keep the first degree with $n = 1$ of the series and ignore other higher degrees, GOA is presented. As mentioned above, GOA may lead to potential errors, so we do not use GOA in this paper.

Now consider the integral $\int_0^{+\infty}\kappa^{2n+1}\Phi_n(\kappa)\mathrm{d}\kappa$ in Eq. (10). Substituting Eq. (5) into Eq. (10), it follows that

$$\int_0^{+\infty}\kappa^{2n+1}\Phi_n(\kappa)\mathrm{d}\kappa = A(\alpha)C_n^2\zeta_\mathrm{e}^{2-\alpha}\int_0^{+\infty}\kappa^{2n+1}\left(\kappa^2+\frac{\kappa_\mathrm{L}^2}{\zeta_\mathrm{e}^2}\right)^{-\frac{\alpha}{2}}\exp\left(-\frac{\zeta_\mathrm{e}^2\kappa^2}{\kappa_\mathrm{H}^2}\right)\mathrm{d}\kappa \tag{11}$$

Using the equation for $p > -1$, $a > 0$ and $b > 0$ [19, 20]

$$\int_0^{+\infty}x^p(x^2+a^2)^q\exp(-b^2x^2)\mathrm{d}x = \frac{1}{2}a^{p+1+2q}\Gamma\left(\frac{p+1}{2}\right)U\left(\frac{p+1}{2};\ \frac{p+3}{2}+q;\ a^2b^2\right) \tag{12}$$

we get

$$\int_0^{+\infty}\kappa^{2n+1}\Phi_n(\kappa)\mathrm{d}\kappa = A(\alpha)C_n^2\zeta_\mathrm{e}^{2-\alpha}\frac{1}{2}\frac{\kappa_\mathrm{L}^{2n+2-\alpha}}{\zeta_\mathrm{e}^{2n+2-\alpha}}\Gamma(n+1)U\left(n+1;\ n+2-\frac{\alpha}{2};\ \frac{\kappa_\mathrm{L}^2}{\kappa_\mathrm{H}^2}\right) \tag{13}$$

where $U(a; c; z)$ is the confluent hypergeometric function of the second kind [18]

$$U(a;\ c;\ z) = \frac{1}{\Gamma(a)}\int_0^{+\infty}\exp(-zt)\,t^{a-1}(1+t)^{c-a-1}\mathrm{d}t \tag{14}$$

Substituting Eq. (13) into Eq. (10), T takes the form as

$$T = -2LA(\alpha)C_n^2 k^2 \pi^2 \kappa_{\mathrm{L}}^{2-\alpha} \times \sum_{n=1}^{+\infty} \frac{\Gamma(n+1)}{(2n+1)n!}\left(-\frac{L\Lambda\kappa_{\mathrm{L}}^2}{k\zeta_{\mathrm{e}}^2}\right)^n U\left(n+1;\ n+2-\frac{\alpha}{2};\ \frac{\kappa_{\mathrm{L}}^2}{\kappa_{\mathrm{H}}^2}\right) \tag{15}$$

In general, it is difficult to obtain the exact close-form expression of Eq. (15). However, an approximate expression can be obtained by the asymptotic behavior of $U(a; c; z)$.

For the real atmospheric turbulence, l_0 is in the order of magnitude of millimeter while L_0 is in the order of magnitude of meter. Thus, the following condition is usually satisfied [1]

$$\frac{\kappa_{\mathrm{L}}^2}{\kappa_{\mathrm{H}}^2} \sim \frac{l_0^2}{L_0^2} \ll 1 \tag{16}$$

Using the property for $|z| \ll 1$ [18]

$$U(a;\ c;\ z) \approx \frac{\Gamma(1-c)}{\Gamma(1+a-c)} + \frac{\Gamma(1-c)}{\Gamma(a)} z^{1-c} \tag{17}$$

we get

$$U\left(n+1;\ n+2-\frac{\alpha}{2};\ \frac{\kappa_{\mathrm{L}}^2}{\kappa_{\mathrm{H}}^2}\right) \approx \frac{\Gamma\left(\frac{\alpha}{2}-n-1\right)}{\Gamma\left(\frac{\alpha}{2}\right)} + \frac{\Gamma\left(n+1-\frac{\alpha}{2}\right)}{\Gamma(n+1)}\left(\frac{\kappa_{\mathrm{L}}^2}{\kappa_{\mathrm{H}}^2}\right)^{\frac{\alpha}{2}-n-1} \tag{18}$$

Substituting Eq. (18) into the series of Eq. (15), it follows that

$$\sum_{n=1}^{+\infty} \frac{\Gamma(n+1)}{(2n+1)n!}\left(-\frac{L\Lambda\kappa_{\mathrm{L}}^2}{k\zeta_{\mathrm{e}}^2}\right)^n U\left(n+1;\ n+2-\frac{\alpha}{2};\ \frac{\kappa_{\mathrm{L}}^2}{\kappa_{\mathrm{H}}^2}\right)$$

$$\approx \frac{1}{2\Gamma\left(\frac{\alpha}{2}\right)} \sum_{n=1}^{+\infty} \frac{\Gamma(n+1)\Gamma\left(\frac{\alpha}{2}-n-1\right)}{\left(n+\frac{1}{2}\right)n!}\left(-\frac{L\Lambda\kappa_{\mathrm{L}}^2}{k\zeta_{\mathrm{e}}^2}\right)^n$$

$$+ \frac{1}{2}\left(\frac{\kappa_{\mathrm{H}}^2}{\kappa_{\mathrm{L}}^2}\right)^{1-\frac{\alpha}{2}} \sum_{n=1}^{+\infty} \frac{\Gamma\left(n+1-\frac{\alpha}{2}\right)}{\left(n+\frac{1}{2}\right)n!}\left(-\frac{L\Lambda\kappa_{\mathrm{H}}^2}{k\zeta_{\mathrm{e}}^2}\right)^n \tag{19}$$

Equation (19) can be generalized into the hypergeometric type [18]

$$ {}_PF_Q(a_1, ..., a_P; c_1, ..., c_Q; z) = \sum_{n=0}^{+\infty} \frac{\prod_{p=1}^{P} (a_p)_n}{\prod_{q=1}^{Q} (c_q)_n} \frac{z^n}{n!} \tag{20} $$

where both P and Q are nonnegative integers and no c_q is zero or a negative integer; $(a)_n$ is the Pochhammer symbol defined by

$$ (a)_n = \frac{\Gamma(a+n)}{\Gamma(a)} \tag{21} $$

and consequently

$$ \begin{cases} \Gamma(n+a) = (a)_n \Gamma(a) \\ \dfrac{1}{n+a} = \dfrac{1}{a} \dfrac{(a)_n}{(a+1)_n} \end{cases} \tag{22} $$

Using the Euler's reflection formula for $z \notin Z$, $\Gamma(1-z)\Gamma(z) = \dfrac{\pi}{\sin(\pi z)}$ [18] we get

$$ \Gamma(a-n) = \frac{\pi}{\sin(\pi a)} \frac{(-1)^n}{(1-a)_n \Gamma(1-a)} \tag{23} $$

Substituting Eq. (22) and Eq. (23) into the first series of Eq. (19), it follows that

$$ \begin{aligned} &\sum_{n=1}^{+\infty} \frac{\Gamma(n+1)\Gamma\left(\frac{\alpha}{2} - n - 1\right)}{\left(n + \frac{1}{2}\right) n!} \left(-\frac{L\Lambda\kappa_{\mathrm{L}}^2}{k\zeta_{\mathrm{e}}^2}\right)^n \\ &= \frac{2\pi\left[1 - {}_2F_2\left(1, \frac{1}{2}; \frac{3}{2}, 2 - \frac{\alpha}{2}; \frac{L\Lambda\kappa_{\mathrm{L}}^2}{k\zeta_{\mathrm{e}}^2}\right)\right]}{\sin\left(\frac{\pi\alpha}{2}\right)\Gamma\left(2 - \frac{\alpha}{2}\right)} \end{aligned} \tag{24} $$

Substituting Eq. (22) and Eq. (23) into the second series of Eq. (19), it follows that

$$ \begin{aligned} &\sum_{n=1}^{+\infty} \frac{\Gamma\left(n + 1 - \frac{\alpha}{2}\right)}{\left(n + \frac{1}{2}\right) n!} \left(-\frac{L\Lambda\kappa_{\mathrm{H}}^2}{k\zeta_{\mathrm{e}}^2}\right)^n \\ &= 2\Gamma\left(1 - \frac{\alpha}{2}\right)\left[{}_2F_1\left(1 - \frac{\alpha}{2}, \frac{1}{2}; \frac{3}{2}; -\frac{L\Lambda\kappa_{\mathrm{H}}^2}{k\zeta_{\mathrm{e}}^2}\right) - 1\right] \end{aligned} \tag{25} $$

Thus, the long-term spreading radius W_{lt} for Gaussian wave can be computed by aforementioned equations.

4. Numerical simulations

We analyze the influence of the anisotropic factor ζ_e on the long-term spreading radius W_{lt}. However, the simulations presented here should be regarded as arbitrary examples to indicate the general form of the analyses and subsequent results. Unless specified otherwise, all numerical simulations were conducted with the default settings: $\lambda = 1.55 \times 10^{-6}$ m, $k \approx 4.05 \times 10^6$ rad/m, $L = 1000$ m, $C_n^2 = 10^{-14}$ m$^{3-\alpha}$, $W_0 = 0.1$ m, and $\Lambda_0 = 0.0494$.

Figure 2 depicts the long-term spreading radius W_{lt} for different types of Gaussian waves as a function of the spectral power law α for several pairs of the inner scale l_0 and outer scale L_0. The anisotropic factor was assigned $\zeta_e = 2$ for this example. As shown in Fig. 2, the long-term spreading radius W_{lt} presents parabolic shape and be-

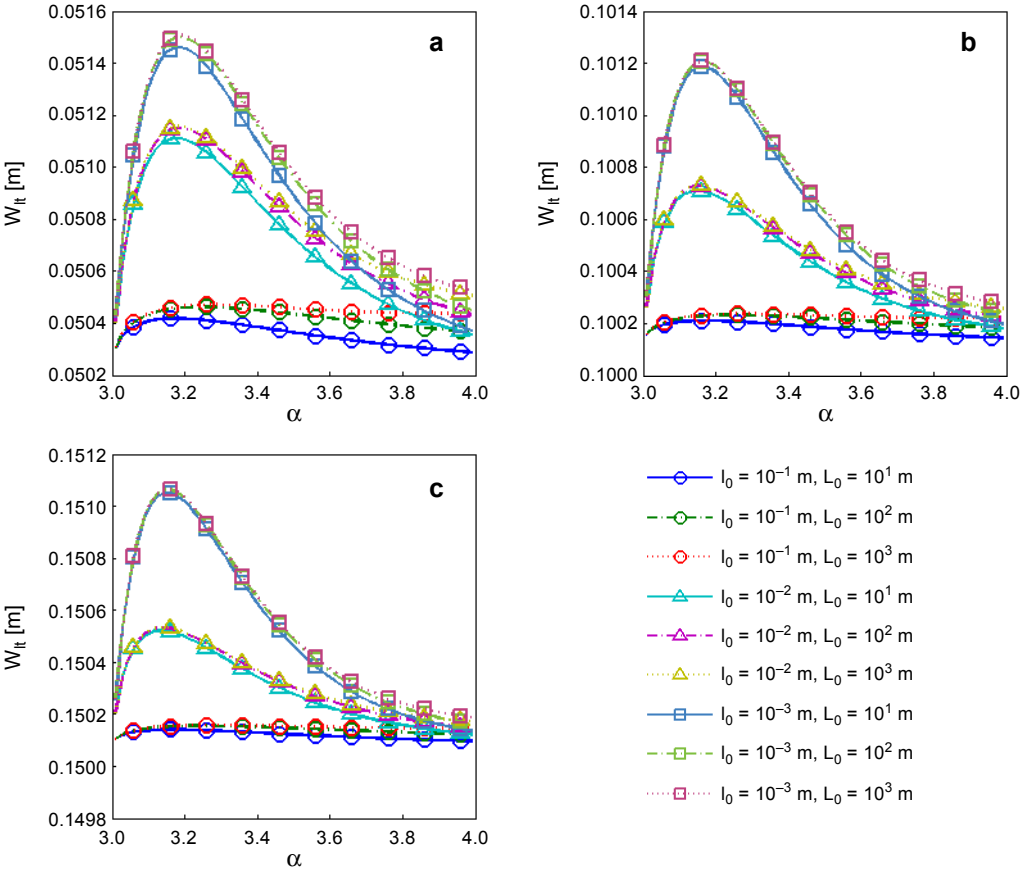

Fig. 2. Long-term spreading radius for different types of Gaussian waves as a function of the spectral power law with several pairs of the inner and outer scale. Convergent beam $\Theta_0 = 0.5$ (**a**), collimated beam $\Theta_0 = 1$ (**b**), and divergent beam $\Theta_0 = 1.5$ (**c**).

comes maximum near $\alpha = 3.2$. Mathematically, $A(\alpha)$ increases monotonically from $\lim_{\alpha \to 3}(\alpha) = 0$ and dominates the calculation of the long-term spreading radius W_{lt} for $3 < \alpha < 3.2$, whereas when $3.2 < \alpha < 4$ the term $\exp(-\zeta_e^2\kappa^2/\kappa_{\mathrm{H}}^2)$ in Eq. (5) takes over, which can be regarded as a low-pass filter about the scalar spatial wave number κ. As mentioned above, the cut-off wave number at high κ_{H} decreases with an increase in the spectral power law α, *i.e.*, larger α allows less turbulence cells to contribute to beam spreading. Figure 2 also indicates that the long-term spreading radius W_{lt} is much more sensitive to the variation of the inner scale l_0 than the outer scale L_0, and increases significantly with a decrease in the inner scale l_0, similar to isotropic turbulence cases. This can be explained by the Richardson cascade theory: the Gaussian wave meets more turbulence eddies along its propagation as the inner scale l_0 decreases, resulting in stronger beam spreading.

For further discussions and analyses, the inner and outer scales of turbulence are assigned to constant values $l_0 = 0.01$ m and $L_0 = 10$ m, respectively. Figure 3 depicts

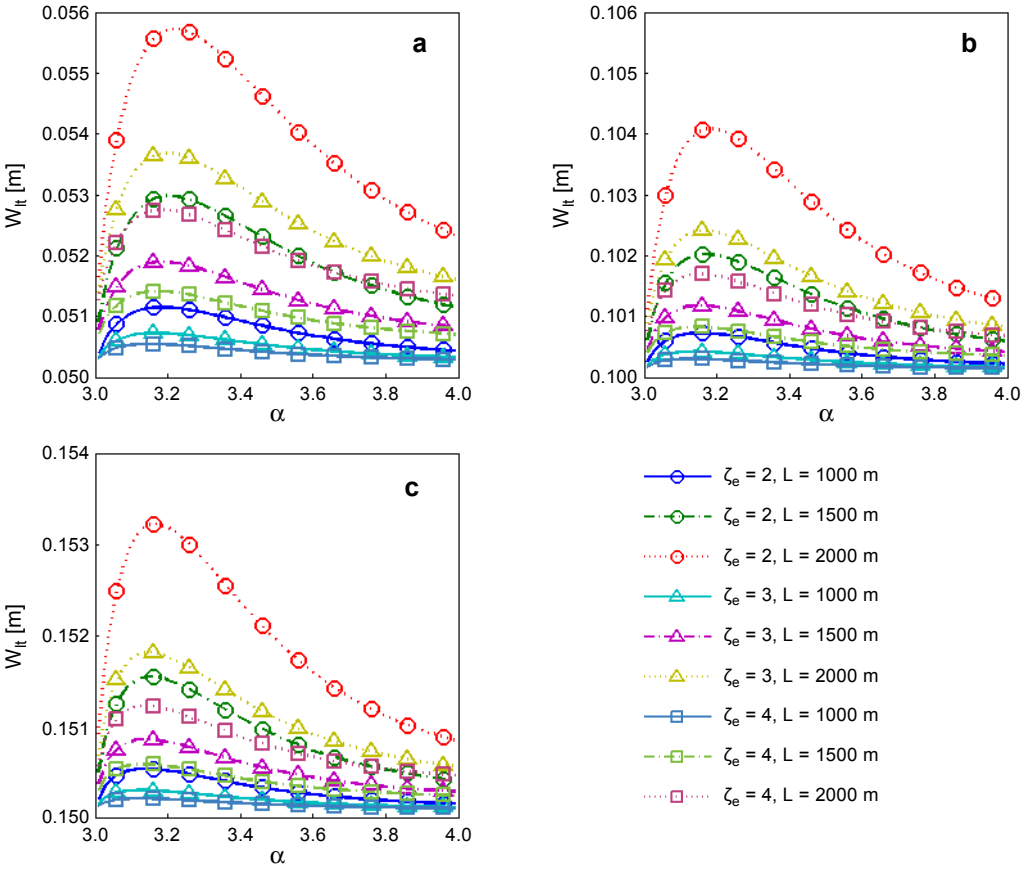

Fig. 3. Long-term spreading radius for different types of Gaussian waves as a function of the spectral power law with several pairs of the anisotropic factor and length. Convergent beam $\Theta_0 = 0.5$ (**a**), collimated beam $\Theta_0 = 1$ (**b**), and divergent beam $\Theta_0 = 1.5$ (**c**).

the long-term spreading radius W_{lt} for different types of Gaussian waves as a function of the spectral power law α for several pairs of the anisotropic factor ζ_e and length L. For the convergent beam ($\Theta_0 = 0.5$) in Fig. 3**a**, as the anisotropic factor ζ_e increases with other parameters fixed, the influence of the anisotropic atmospheric turbulence on the long-term spreading radius W_{lt} reduces significantly. This is similarly the case for the collimated beam ($\Theta_0 = 1$) in Fig. 3**b** and the divergent beam ($\Theta_0 = 1.5$) in Fig. 3**c**. Physically, these phenomena are caused by stochastic fluctuations of curvature among the anisotropic turbulence cells. Acting as lenses with large radii of curvature, these anisotropic turbulence cells can significantly modify the focusing properties of the transmission media. The larger radius of curvature, which means an increasing anisotropic factor ζ_e mathematically, makes the optical beam less deviated from its propagation path. Ultimately, the long-term spreading radius will take smaller value.

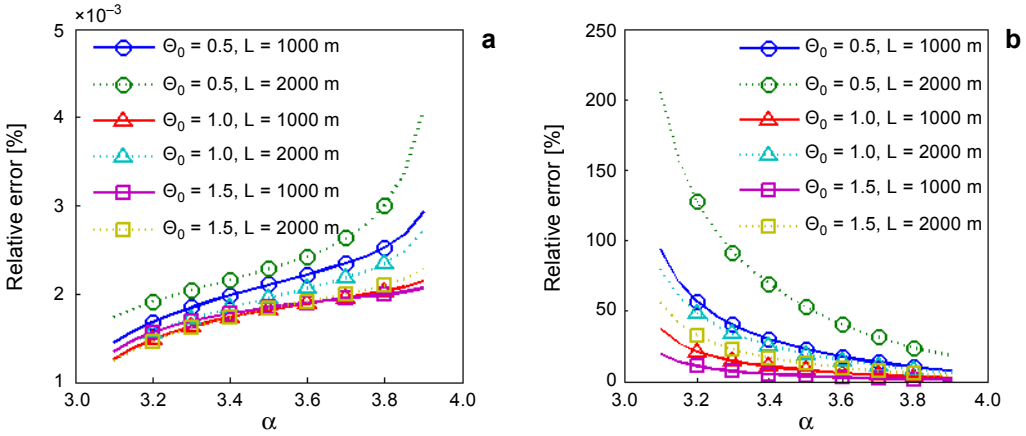

Fig. 4. Relative errors of Eq. (6) using different models as a function of the spectral power law for different Gaussian waves with several length. Our model (**a**), and GOA-based model (**b**).

Figure 4 depicts the relative errors of Eq. (6) as a function of the spectral power law α for our proposed model and the GOA-based model. The exact value of Eq. (6) for each case was computed by numerical integration. It is clear that our proposed model is at least two orders of magnitude more accurate than the GOA-based model. This is particularly the case for the GOA-based model when the spectral power law α approaches 3. Physically, GOA is limited to the situation $l_F \ll l_0$ for classical Kolmogorov turbulence with $\alpha = 11/3$, where the inner scale l_0 corresponds to the cut-off wave number at high κ_H. Thus, we can infer that the GOA-based model should be limited to the situation where the equivalent wave number κ_F of Fresnel's scale l_F is much larger than the cut-off wave number at high κ_H for non-Kolmogorov turbulence. As discussed above, the cut-off wave number at high κ_H increases with a decrease in the spectral power law α. Therefore, the condition $\kappa_F \gg \kappa_H$ may no longer be satisfied near $\alpha = 3$, and errors increase for the GOA-based model.

5. Conclusion

Beam spreading for a Gaussian wave propagating through anisotropic non-Kolmogorov atmospheric turbulence along a horizontal path was investigated. Applying the Markov approximation, the generalized von Kármán spectrum for anisotropic turbulence was utilized to analyze the effects of the anisotropic factor on the long-term spreading radius for different types of Gaussian waves. Approximate expressions were obtained by the asymptotic behavior of the confluent hypergeometric function, as well as the universal type of hypergeometric function. Numerical simulations indicate that anisotropic atmospheric turbulence on beam spreading will decrease with increasing anisotropy. The long-term spreading radius increases significantly with a decrease in the inner scale, which is in accordance with isotropic turbulence cases. We also compared our proposed model and the GOA-based model, and verified that the GOA-based model was inaccurate for a small spectral power law value.

The simulations performed here should only be regarded as examples to illuminate particular cases, and are mainly useful for theoretical analyses. In practice, the anisotropic factor will not always satisfy linear laws, rather obeying parabolic laws on any scales of the turbulence eddy. Furthermore, due to the lack of adequate data and prior information about anisotropic turbulence, the optical parameters used in Section 4 may fail to describe actual atmospheric propagation. Once novel instruments are capable of gathering, the degree of anisotropy at various scales, the expressions deduced here can be generalized to practical whole atmospheric layers.

References

[1] Andrews L.C., Phillips R.L., *Laser-Beam Propagation through Random Media*, 2nd Ed., SPIE Optical Engineering Press, Bellingham, 2005.

[2] Jun Zeng, Jinhong Li, *Dynamic evolution and classification of coherent vortices in atmospheric turbulence*, Optica Applicata **45**(3) 2015, pp. 299–308.

[3] Guohua Wu, Bin Luo, Song Yu, Anhong Dang, Tonggang Zhao, Hong Guo, *Effects of coherence and polarization on the beam spreading and direction through atmospheric turbulence*, Optics Communications **284**(19), 2011, pp. 4275–4278.

[4] Wenhe Du, Hengjun Zhu, Daosen Liu, Zhongmin Yao, Chengjiang Cai, Xiufeng Du, Ruibo Ai, *Effect of non-Kolmogorov turbulence on beam spreading in satellite laser communication*, Journal of Russian Laser Research **33**(5), 2012, pp. 456–463.

[5] Kolmogorov A.N., *The local structure of turbulence in incompressible viscous fluid for very large Reynolds numbers*, Proceedings of the Royal Society A **434**(1890), 191, pp. 9–13.

[6] Toselli I., Andrews L.C., Phillips R.L., Ferrero V., *Free-space optical system performance for laser beam propagation through non-Kolmogorov turbulence*, Optical Engineering **47**(2), 2008, article ID 026003.

[7] Chao Gao, Yang Li, Yiming Li, Xiaofeng Li, *Irradiance scintillation index for a Gaussian beam based on the generalized modified atmospheric spectrum with aperture averaged*, International Journal of Optics, Vol. 2016, 2016, article ID 8730609.

[8] Consortini A.A., Ronchi L., Stefanutti L., *Investigation of atmospheric turbulence by narrow laser beams*, Applied Optics **9**(11), 1970, pp. 2543–2547.

[9] DALAUDIER F., SIDI C., CROCHET M., VERNIN J., *Direct evidence of "sheets" in the atmospheric temperature field*, Journal of the Atmospheric Sciences **51**(2), 1994, pp. 237–248.
[10] TOSELLI I., AGRAWAL B., RESTAINO S., *Light propagation through anisotropic turbulence*, Journal of the Optical Society of America A **28**(3), 2011, pp. 483–488.
[11] TOSELLI I., *Introducing the concept of anisotropy at different scales for modeling optical turbulence*, Journal of the Optical Society of America A **31**(8), 2014, pp. 1868–1875.
[12] ANDREWS L.C., PHILLIPS R.L., CRABBS R., *Propagation of a Gaussian-beam wave in general anisotropic turbulence*, Proceedings of SPIE **9224**, 2014, article ID 922402.
[13] TOSELLI I., KOROTKOVA O., *General scale-dependent anisotropic turbulence and its impact on free space optical communication system performance*, Journal of the Optical Society of America A **32**(6), 2015, pp. 1017–1025.
[14] TOSELLI I., KOROTKOVA O., *Spread and wander of a laser beam propagating through anisotropic turbulence*, Proceedings of SPIE **9614**, 2015, article ID 96140B.
[15] FEINAN CHEN, JINGJING CHEN, QI ZHAO, YANRU CHEN, YU XIN, JIA LI, HUA PAN, *Spectral degrees of cross-polarization of stochastic anisotropic electromagnetic beams in modified non-Kolmogorov atmospheric turbulence*, Optica Applicata **43**(4), 2013, pp. 773–783.
[16] LINYAN CUI, BINDANG XUE, FUGEN ZHOU, *Generalized anisotropic turbulence spectra and applications in the optical waves' propagation through anisotropic turbulence*, Optics Express **23**(23), 2015, pp. 30088–30103.
[17] CHAO GAO, LINGLING SU, WANKE YU, *Long-term spreading of Gaussian beam using generalized modified atmospheric spectrum*, The 12th IEEE International Conference on Mechatronics and Automation, August 2–5, 2015, Beijing, China, IEEE, pp. 2375–2380.
[18] OLVER F.W.J., LOZIER D.W.L., BOISVERT R.F., CLARK C.W., *NIST Handbook of Mathematical Functions*, Cambridge University Press, New York, 2010.
[19] ERDELYI A., MAGNUS W., OBERHETTINGER F., *Tables of Integral Transforms, McGraw-Hill*, New York, 1954.
[20] GRADSHTEYN I.S., RYZHIK I.M., *Table of Integrals, Series, and Products*, 8th Ed., Academic Press, Waltham, 2014.

Received May 28, 2016
in revised form July 11, 2016